sciendo

Geologos 28, 1 (2022): 19–37
DOI: 10.2478/logos-2022-0002

GEOLOGOS

Tectonomagmatic settings of Jurassic granitoids in the Sanandaj-Sirjan Zone, Iran: A review

Mohammad Hassan Karimpour[1, 2]*, Nargess Shirdashtzadeh[3], Martiya Sadeghi[4]

[1] Research Center for Ore Deposits of Eastern Iran, Faculty of Science, Ferdowsi University of Mashhad, Mashhad, Iran
[2] Department of Geological Sciences, University of Colorado, Boulder, USA; e-mail: karimpom@colorado.edu
[3] Department of Geology, University of Isfahan, P.O. Box: 8174673441, Isfahan, Iran; e-mail: nshirdasht@gmail.com
[4] Mineral Resource Department, Geological Survey of Sweden, Uppsala, Sweden; e-mail: martiya.sadeghi@sgu.se
*corresponding author, e-mail: karimpur@um.ac.ir

Abstract

The present paper discusses the geochemical affinities, origin and ages of Jurassic granitoids of the Sanandaj-Sirjan Zone (SaSZ) in the eastern part of the Zagros Thrust Zone. A multidisciplinary, integrated approach was carried out using existing granitoid geochemical data (major, trace, rare earth element and isotopes) and knowledge of the regional geology (geodynamic and metamorphic setting), coupled with geophysical data (magnetic susceptibility) from granitoids in the SaSZ. We re-interpret and re-classify the Jurassic granitoids of this zone into three main genetic groups: S-type, I-type and A-type subduction-related ones. In the central to southern part of the Sanandaj-Sirjan zone (between Hamadan and Sirjan), S-type magmatism appeared between 178 and 160 Ma during the Cimmerian orogeny, due to continental collision. To the north of the Sanandaj-Sirjan zone (between Sanandaj and Ghorveh), I-type and A-type magmatism occurred between 158 and 145 Ma. This heterogenic tectonomagmatic system along the SaSZ suggests a heterogenic subcontinental lithospheric mantle, resulting in two Jurassic tectonomagmatic zones of (1) the Sanandaj-Ghorveh Zone and (2) the Hamadan-Sirjan Zone.

Key words: Geochemical data, geophysical data, Jurassic magmatism, Sanandaj-Ghorveh Zone, Hamadan-Sirjan Zone

1. Introduction

The Zagros Orogen is a central segment (at the tectonic crossroads) of the gigantic Alpine-Himalayan convergence zone that extends from the western Mediterranean region through northern Iraq and the northwest of Iran to the Hormuz Strait, Oman and Himalayas (e.g., Agard et al., 2005; Ajirlu et al., 2016). As a consequence of rifting and closure episodes of Neo-Tethyan oceanic crust between the Arabia block and the Sanandaj-Sirjan Zone (SaSZ) during the Zagros Orogen (e.g., Berberian & King, 1981; Alavi, 1994; Mohajjel et al., 2003; Ghasemi & Talbot, 2006; Mohajjel & Fergusson, 2014; Fergusson et al., 2016), the SaSZ was deformed. A series of metamorphic-magmatic rocks were emplaced in the eastern part of a thrust fault in Zagros (e.g., Mehdipour Ghazi & Moazzen, 2015), to the east of the Main Thrust Fault. The SaSZ (Fig. 1) is therefore a metamorphic–magmatic belt that is characterised by metamorphosed and deformed rocks with Mesozoic calc-alkaline plutons and lavas (Agard et al., 2011). Basement metamorphic, igneous and sedimentary rocks are interpreted to form the

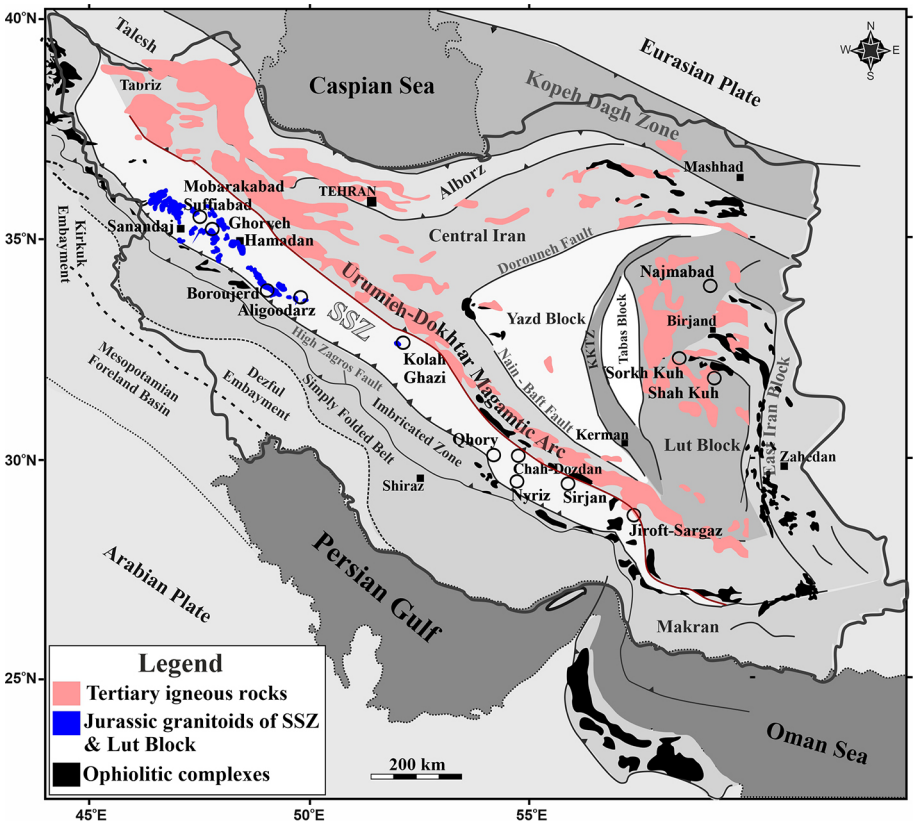

Fig. 1. Simplified geological map of Iran and the Zagros Orogen, modified after Le Garzic et al. (2019).

southwestern margin of the Cimmerian continental fragment (Ricou, 1994; Stampfli & Borel, 2002; Fergusson et al., 2016).

Jurassic intrusive rocks show a wide distribution along the SaSZ from Sanandaj to Sirjan regions (Fig. 1). Several geochemical and geochronological studies carried out on the Jurassic intrusive rocks of SaSZ (e.g., Shahbazi et al., 2010; Azizi et al., 2011; Esna-Ashari et al., 2012; Chiu et al., 2013; Yajam et al., 2015; Bayati et al., 2017; Yang et al., 2018; Azizi et al., 2020a) have provided valuable geochemical and geochronological data for the interpretation of the tectonomagmatic pattern of SaSZ. However, current tectonomagmatic models proposed for the origin of Jurassic magmatism of SaSZ are controversial.

The widely accepted models ascribe the SaSZ Jurassic magmatism to (1) a slab window within the subducting Neo-Tethys slab beneath an Andean-like continental active margin of the SaSZ causing partial melting of overlying continental lithospheric material (e.g., Khalaji et al., 2007; Sepahi et al., 2014; Abdulzahra et al., 2018; Deevsalar et al., 2018; Yang et al., 2018; Zhang et al., 2018a; Daneshvar et al., 2019), or (2) a subduction-related continental rift (e.g., Azizi et al., 2017; Azizi & Stern, 2019; Azizi et al., 2020a, 2020b; Tavakoli et al., 2020). Karimpour et al. (2021) suggested that the SaSZ granitoids from Hamedan to Sirjan (Fig. 1) formed by melting of a continental crust in a collisional zone during the Cimmerian orogeny and are S-type granitoids with no tin mineralisation.

Our review aims to revisit and discuss the magmatic events and the tectonomagmatic setting of the SaSZ. Our focus is on the comparison of Jurassic northern SaSZ granitoids (from Sanandaj-Ghorveh-Dehgolan to Hamedan) with Jurassic central and southern granitoids (from Hamedan to Sirjan). The topic was previously discussed, in Persian, by Karimpour et al. (2021). We here use compiled published geochemical, isotopic and geochronological data for the Jurassic granitoids from northern, central and southern SaSZ and integrate them with airborne magnetic data to present an extensive reinterpretation of the geochemical affinities, origins and ages of various Jurassic granitoid intrusive rocks of the Sanandaj-Sirjan Zone.

There have been many attempts to correlate different granitoid compositions and geotectonic environments by using major, trace and rare earth elements (e.g., Pearce et al., 1984; Chappell & White, 2001; Chappell, 2004; Chappell et al., 2004; Gill, 2010; Clemens et al., 2011; Clemens & Stevens, 2012; Grebennikov, 2014). Initial Nd and Sr isotopic compositions are also commonly used to determine

various types and origins of granitoids (e.g., McCulloch & Chappell, 1982; Gill, 2010). On the basis of magnetic minerals, granitic rocks can be divided into two series: (1) a magnetite and/or magnetite-ilmenite series, and (2) an ilmenite series (Ishihara 1977). This may, hypothetically, correspond basically to I- and /or A-types, while the weakly magnetic granites correspond to the S-type (Takahashi et al., 1980; Ellwood & Wenner, 1981). Based upon these classifications, SaSZ granitoids can be divided into several types, which are suggested to correspond to different tectonic environments.

2. Geological background of the SaSZ

As a consequence of a complex geological history, Iran is an amalgamation of various structural units including the Zagros Orogen, Kopet Dagh Zone, Central Iran (with the Central-East Iranian Microcontinent, including Yazd block, Kerman-Kashmar tectonic zone, Tabas and Lut blocks), Eastern Iran and the Makran Zone (Fig. 1). The Zagros Orogen is subdivided into several NW–SE trending, parallel subzones of the Mesopotamian–Persian Gulf Foreland, the Dezful Embayment, the Zagros Simply Folded Belt, the Zagros Thrust Belt, the Crush Zone (High Zagros or Imbricated Zone), the ophiolitic Zagros Outer Belt, the Sanandaj-Sirjan Zone (SaSZ) and the Urumieh–Dokhtar Magmatic Arc (e.g., Chiu et al., 2013; Mohajjel & Fergusson, 2014; Ajirlu et al., 2016; see Fig. 1). Previous researchers have proposed several subdivisions of the Zagros Orogen and presented interpretations on timing and position of the suture zone based on tectonomagmatic and structural features (e.g., Alavi, 2007; Homke et al., 2010; Agard et al., 2011 and references therein; Chiu et al., 2013; Mohajjel & Fergusson, 2014; Ajirlu et al., 2016.). In addition to the scattered fragments of Gondwanan basement outcrops [e.g., northwest of SaSZ (551–544 Ma; Hassanzadeh et al., 2008), Saqqez (559–547 Ma; Daneshvar et al., 2019), Soursat (537 Ma; Jamshidibadr et al., 2013), Muteh (578–596 Ma; Hassanzadeh et al., 2008), Azna (526 Ma; Shabanian et al., 2018), Gol-Gohar (555 Ma; Safarzadeh et al., 2016)], the SaSZ represented an active Andean-like Mesozoic margin with metamorphism and calc-alkaline magmatic activity progressively shifted northwards during most of the second half of the Mesozoic (Berberian & King, 1981; Agard et al., 2005, 2011). Thus, this tectonic zone is characterised by several magmatic pulses and polymetamorphic episodes varying from the northern to southern parts of SaSZ. It is divided into three subzones from the north to the south (Azizi & Stern, 2019). The northern SaSZ (N-SaSZ) consists of igneous and metamorphic rocks (500–600 Ma) and Palaeozoic granite along with mafic to intermediate Cretaceous volcanic rocks (Azizi & Jahangiri, 2008; Azizi et al., 2017) interbedded with Mesozoic shales. The central part of SaSZ (C-SaSZ) consists of Cadomian basement, mainly deformed amphibolite and granites, regional high-grade metamorphic rocks of Early to mid-Jurassic age (Baharifar et al., 2004), and mafic to felsic intrusive rocks. The southern part of SaSZ (S-SaSZ) is mainly composed of Palaeozoic metamorphic rocks overlain by non-metamorphosed Triassic and Jurassic sedimentary rocks (Sheikholeslami, 2015).

2.1. Metamorphism of the SaSZ

The metamorphic lithological composition of the SaSZ includes slates, phyllites and schists, originating from shales formed in a continental island arc tectonic setting during the Zagros orogeny (Hemmati et al., 2018). The Zagros Orogen is defined by several regional metamorphic episodes in the Mesozoic (~ >170 Ma and ~ 145 Ma) and Cenozoic (~80–70 Ma and ~50–32 Ma) recorded in various metamorphic and magmatic rocks of this collisional zone, especially from the Hamedan to Ghorveh areas:

- In the N-SaSZ, two magmatic pulses and polymetamorphic episodes imprint on Hamadan high-grade metapelites (Fergusson et al., 2016; Monfaredi et al., 2020) and on the Ghorveh area (Azizi et al., 2018) in the following order: (1) relic metamorphism predating pluton emplacement in the Early Jurassic (Monfaredi et al., 2020); (2) a Cimmerian orogenic episode in the Early to Middle Jurassic affected the Sanandaj–Sirjan Zone, confirmed by U-Pb dating of detrital zircons in the Hamadan phyllite (Fergusson et al., 2016); (3) a contact metamorphic overprint (hornfels: 168 ± 11 Ma; T: ~ 560 and 660°C; P: ~ 2.7 kbar; Monfaredi et al., 2020) formed during the emplacement of the Alvand composite pluton (between 171.1 ± 1.2 and 153.3 ± 2.7 Ma; e.g., Shahbazi et al., 2010; Mahmoudi et al., 2011; Sepahi et al., 2018); (4) low-grade greenschist-amphibolite facies metamorphism is shown by both schistose rocks of Hamedan (149 ± 19 Ma; T: 490 and 690°C; P: 3.5–5.5 kbar; Monfaredi et al., 2020) and the Ghalaylan submarine metabasites (145–144 Ma; Azizi et al., 2018) in the Ghorveh area. The schistose rocks, interlayered with marble, were metamorphosed at lower greenschist facies (Azizi et al., 2018), and (5) a Buchan-type regional metamorphic event marked by $^{40}Ar/^{39}Ar$ ages in the 80–70 Ma range (Late Cretaceous).

- In the C-SaSZ, the thermochronological studies in the Dorud-Azna region by Shakerardakani et al. (2015) have revealed (1) an Early Jurassic amphibolite-grade metamorphism with ductile fabrics predating 170 Ma (>170 Ma), caused by the accretion of the SaSZ basement to central Iran, and (2) an Eocene metamorphic overprint at around 50–32 Ma during the emplacement of amphibolite-meta-gabbro unit over the June complex and Galeh-Doz orthogneiss.
- In the S-SaSZ, the Palaeozoic and Mesozoic rocks were affected by at least two syn-metamorphic regional deformations (Sheikholeslami, 2015) including (1) an early Cimmerian metamorphic event altering Palaeozoic rocks into gneiss, schist, marble and amphibolite. This event is truncated by an angular unconformity separating Palaeozoic metamorphic rocks from Jurassic turbiditic rocks, which were partly deformed and metamorphosed under greenschist facies condition (Sheikholeslami, 2015); (2) The second regional deformation event (characterised by the deformation of bedding, folding and reorientation of pre-existing structures, spaced cleavage, kinks and microfolds formed in brittle-ductile conditions) caused the deformation of early Cimmerian event rocks and metamorphism of the turbidites.

2.2. Magmatism in the SaSZ

The SaSZ is composed of magmatic rocks of Precambrian (~550 Ma; Hassanzadeh et al., 2008; Jamshidibadr et al., 2013; Daneshvar et al., 2019), Palaeozoic (320 Ma, Moghadam et al., 2015; 360 Ma, Azizi et al., 2017, 520–513 Ma, Badr et al., 2018),

Table 1. Age of and isotopic data for Jurassic granitoid rocks in the Sanandaj-Sirjan Zone.

Location	Rock type	U-Pb Age (Ma)	$(^{87}Sr/^{86}Sr)_i$	$(^{143}Nd/^{144}Nd)_i$	εNd_i	Granitoid	T_{DM}	Reference
South Ghorveh	Diorite	150	0.70622	0.512625	3.5	A-Type	937	Zhang et al. (2018a)
		150	0.70489	0.512564	2.3		967	
	Monzonite	146	0.70555	0.512393	−1.1		1068	
		146	0.70552	0.512385	−1.2		1053	
		146	0.70615	0.512375	−1.4		1126	
Bolbanabad	Diorite	146	0.70369	0.512725	5.4	A-Type	619	Zhang et al. (2018a)
	Granite	146	N.A.	0.512579	2.5		726	
		146	N.A.	0.512588	2.7		657	
		146	N.A.	0.512585	2.6		753	
Mobarakabad	Monzonite	147	0.70369	0.512725	5.4	I-Type	619	Zhang et al. (2018a)
		148	N.A.	N.A.	N.A.		N.A.	
			0.70300	0.512710	4.4		575	Azizi & Asahara (2013)
			0.70430	0.512660	3.4		727	
	Monzonite		0.70430	0.512710	4.0		730	
			0.70330	0.512620	3.1		769	
			0.70340	0.512650	3.6		736	
Ghalaylan	Granite	158	0.70426	0.512470	0.6	I-Type	767	Azizi et al. (2015b)
		158	0.70430	0.512490	0.9		585	
		158	0.70447	0.512460	0.4		700	
		158	0.70447	0.512520	1.4		592	
		158	0.70465	0.512500	1.0		598	
	Monzonite Granite	156	0.70441	0.512490	0.9		641	
		156	0.70456	0.512500	1.1		585	
		156	0.70450	0.512480	0.7		617	
		156	0.70452	0.512520	1.4		329	
		156	0.70453	0.512400	−0.8		803	
Suffiabad	Granite	148	0.70410	0.512570	2.3	I-Type	928	Azizi et al. (2011)
		145	0.70240	0.512700	4.9		711	
		145	0.70280	0.512560	2.2		820	
	Diorite	145	0.70500	0.512650	3.9		326	
	Granite	145	0.70530	0.512610	3.2		1805	
		145	0.70550	0.512530	1.5		909	

Location	Rock type	U-Pb Age (Ma)	$(^{87}Sr/^{86}Sr)_i$	$(^{143}Nd/^{144}Nd)_i$	εNd_i	Granitoid	T_{DM}	Reference
Shirvaneh	Diorite	154	0.70518	0.512570	2.3	I-Type	791	Azizi et al. (2020b)
		152	0.70563	0.512520	1.4		872	
		146	0.70352	0.512510	1.3		847	
		146	0.70472	0.512610	3.2		813	
Ghorveh-Dehgolan	Monzonite	150	0.70404	0.512569	2.5		604	Yajam et al. (2015)
W Hamadan	Granite	171	N.A.	N.A.	N.A.	S-Type	N.A.	Zhang et al. (2018b)
		168	N.A.	N.A.	N.A.		N.A.	
S Hamadan	Granite	167	N.A.	N.A.	N.A.	S-Type	N.A.	
Alvand (Hamadan)	Leucogranite	165	N.A.	N.A.	N.A.	S-Type	N.A.	Chiu et al. (2013)
		164	N.A.	N.A.	N.A.		N.A.	
	Granite	163–161	0.71938	0.512257	−3.3		1200	Shahbazi et al. (2010)
		163–161	0.70924	0.512312	−2.3		1130	
	Granite	164	0.70883	0.512252	−3.4		1220	
	Granite	161	0.70699	0.512375	−1.1		1030	
	Granite	154	0.71301	0.512260	−3.5		1230	
		154	0.71377	0.512210	−4.5		1310	
		154	0.71273	0.512259	−3.5		1230	
Malayer	Syenogranite	184	0.70944	0.512230	−3.4	S-Type	1132	Ahadnejad et al. (2011)
		184	0.71087	0.512190	−4.3		1269	
	Diorite	174	0.70856	0.512280	−2.7		955	
	Granodiorite	170	0.70921	0.512260	−2.6		1124	
		170	0.70855	0.512230	−3.7		1152	
	Tonalite	169	0.70877	0.512300	−2.3		1092	
	Monzogranite	162	0.70797	0.512160	−4.9		1330	
		162	0.70858	0.512190	−4.6		1252	
Astaneh (Shazand)	Granodiorite	171	0.70824	0.512124	−5.8	S-Type	1370	Tahmasbi et al. (2010)
	Qtz-diorite	171	0.70842	0.512143	−5.4		1350	
		171	0.70804	0.512110	−6.0		1390	
Nezam Abad (Boroujerd)	Monzogranites	172	0.70630	0.51226	−3.0	S-Type	1006	Khalaji et al. (2007)
	Granodiorite	172	0.70660	0.51225	−3.3		869	
		171	0.70660	0.51224	−3.5		867	
	Quartz diorite	171	0.70620	0.51223	−3.6		1135	
		170	0.70740	0.51226	−3.1		1269	
Aligoodarz	Granodiorite	170	N.A.	N.A.	N.A.	S-Type	N.A.	Zhang et al. (2018b)
		167	N.A.	N.A.	N.A.		N.A.	
		165	0.71010	0.51214	−5.5		1450	Esna-Ashari et al. (2012)
		165	0.71010	0.51215	−5.4		1410	
		165	0.70970	0.51218	−4.8		1530	
	Granite	165	0.71100	0.51216	−5.3		2420	
Kolah-Ghazi	Monzogranite	167–175	N.A.	N.A.	N.A.	S-Type	N.A.	Bayati et al. (2017)
	Granite	165	N.A.	N.A.	N.A.		N.A.	Chiu et al. (2013)
Qhory (Neyriz)	Granite	175	N.A.	N.A.	N.A.	S-Type	N.A.	Yang et al. (2018)
		173	N.A.	N.A.	N.A.		N.A.	
		170	N.A.	N.A.	N.A.		N.A.	
Jiroft-Sargaz	Granite	175	N.A.	N.A.	N.A.	S-Type	N.A.	Chiu et al. (2013)

Jurassic (178–145 Ma; e.g., Khalaji et al., 2007; Tahmasbi et al., 2010; Ahadnejad et al., 2011; Mahmoudi et al., 2011; Azizi & Asahara, 2013; Hunziker et al., 2015; Azizi et al., 2015b; Zhang et al., 2018a, 2018b; Azizi & Stern, 2019), Cretaceous (109 Ma, Mahmoudi et al., 2011; 111.6 Ma, Abdulzahra et al., 2018) to Paleogene (~40 Ma, Mazhari et al., 2009; 60 Ma, Mahmoudi et al., 2011; 38 Ma, Sepahi et al.,

2014). These lithologies (e.g., Jurassic – see Table 1) include mafic to acidic intrusive rocks, mainly classified as collisional and post-collisional I- and S-types, and minor A-types and H-type (hybrid) rocks, formed in the continental active margin of a subduction-related tectonomagmtic setting (e.g., Khalaji et al., 2007; Sepahi et al., 2014; Abdulzahra et al., 2018; Deevsalar et al., 2018; Daneshvar et al., 2019) and intra-continental rifting (Azizi et al., 2017; Azizi et al., 2020a; Tavakoli et al., 2020).

The distribution of Precambrian granitoids in SaSZ is related to an active Peri-Gondwanan continental margin of the Proto-Tethys Ocean (Hassanzadeh et al., 2008; Daneshvar et al., 2019). The younger (Jurassic to Paleogene) magmatic rocks are mostly ascribed to the Andean-like continental active margin of the SaSZ during the Neo-Tethys subduction.

3. Data and material

Published geochemical (102 major, trace and rare earth element analyses), isotopic (50 $^{87}Sr/^{86}Sr_i$, and 64 εNd_i analyses), geochronological (46 U-Pb zircon ages) and geophysical data (airborne magnetic intensity) for the SaSZ Jurassic granitoids were compiled and integrated (Tables 1 and 2). "Intermediate to acidic" rock types (e.g., granite, monzonite, diorite, tonalite) were selected from the S- to N-SaSZ (i.e., South Ghorveh, Bolbanabad, Mobarakabad, Ghalaylan, Suffiabad, Shirvaneh, Ghorveh-Dehgolan, W Hamadan, South Hamadan, Alvand (Hamadan), Malayer, Astaneh (Shazand), Nezam Abad (Boroujerd), Aligoodarz, Kolah-Ghazi, Qhory (Neyriz) and Jiroft-Sargaz areas) (Fig. 1). We only considered zircon U-Pb ages and isotopic (Sr and Nd) and geochemical data (major, trace and rare earth elements) obtained by comparable, high-quality sample preparations (e.g., lithium metaborate fusion) and modern analytical methods (e.g., XRF, ICP-MS, LA-ICP-MS of U-Pb zircon, etc.). The aeromagnetic and magnetic susceptibility map of Iran is adopted from Teknik & Ghods (2017).

Table 2. Geochemistry of Jurassic granitoids in the Sanandaj-Sirjan Zone. Contents of trace elements in ppm.

Location	Age (Ma)	$(^{87}Sr/^{86}Sr)_i$	εNd_I	Rb	Sr	Y	Ba	$(Eu/Eu)_N$	References
Mobarakabad (Iran)	147–148	0.703	4.4	71	86	35	291	0.711	Azizi & Asahara (2013); Zhang et al. (2018a)
			3.4	104	93	44	394	1.28	
			4.0	19	188	41	171	1.04	
			3.1	46	221	29	138	0.948	
			3.6	17	207	29	149	1.004	
Shirvaneh (Iran)	146–154	0.705	2.3	63	217	55	419	1.137	Azizi et al. (2020b)
			1.4	115	170	35	604	0.566	
			1.3	186	66	40	454	0.57	
			3.2	75	221	29	402	0.997	
Suffiabad (Iran)		0.704	2.3	112	33	18	244	0.853	Azizi et al. (2011)
			4.9	101	59	25	279	1.28	
			2.2	99	37	31	222	2.133	
			3.9	62	388	24	362	1.673	
			3.2	39	33	17	71	1.589	
			1.5	35	34	4	14	2.686	
Ghalaylan (Iran)	156–158	0.705	0.6	126	1198	16	1176	2.364	Azizi et al. (2015b)
			0.9	96	845	11	1186	1.407	
			0.4	112	778	13	1042	2.18	
			1.4	101	452	12	940	2.814	
			1.0	63	915	11	1164	1.38	
			0.9	141	1128	20	1106	1.844	
			1.1	77	1083	9	1327	1.493	
			0.7	62	813	16	1004	1.609	
			1.4	128	1013	20	1039	1.768	
			−0.8	151	1639	11	1577	2.339	
Bolbanabad (Iran)	146	0.704	5.4	31	225	38	274	0.740	Zhang et al. (2018a)
			2.5	176	40	40	306	0.423	
			2.6	165	31	44	321	0.307	
			2.7	160	37	41	281	0.411	

Location	Age (Ma)	$(^{87}Sr/^{86}Sr)_i$	εNd_t	Rb	Sr	Y	Ba	$(Eu/Eu)_N$	References
South Ghorveh (Iran)	146–150	0.706	3.5	18	347	44	56	1.523	Zhang et al. (2018a)
			2.3	36	365	39	111	1.739	
			−1.1	106	102	62	753	1.036	
			−1.2	114	99	63	696	0.92	
			−1.4	105	117	68	773	0.985	
W-Hamadan (Iran)	168			194	245	30	729	0.582	Zhang et al. (2018b)
				161	418	32.7	765	0.631	
				167	294	33.5	129	0.573	
				180	91	20.8	212	0.375	
				163	167	26.2	469	0.406	
				166	170	19.8	460	0.341	
				175	168	21.1	480	0.582	
Malayer (Iran)	170	0.709	−3	134	320	15	1150	0.391	Ahadnejad et al. (2011)
				88	347	23.4	355	0.447	
				77	231	30.2	361	0.457	
				87	142	42	162	0.339	
				96	160	17.7	292	0.774	
				86	141	16.9	286	0.719	
Aligoodarz (Iran)	165	0.71	−5	137	113	20.9	345	0.494	Esna-Ashari et al. (2012); Zhang et al. (2018b)
				104	192	37.4	348	0.257	
				141	124	27.1	347	0.370	
				130	138	23.1	291	0.556	
				166	146	22	406	0.517	
				151	107	29.3	401	0.546	
				137	113	20.9	345	0.494	
				104	192	37.4	348	0.323	
				82	206	23.6	259	0.487	
Alvand (Iran)	167–171	0.709–0.710	−3	163	134	44	387	0.287	Zhang et al. (2018b); Chiu et al. (2013); Shahbazi et al. (2010)
				148	151	10.9	667	0.473	
				248	140	54.4	178	0.534	
				190	160	17	130	0.616	
				198	160	27.3	800	0.252	
Boroujerd (Iran)	169.6	0.708	−3.5	79	197	18.4	236	0.671	Khalaji et al. (2007)
				101	388	19.8	454	0.648	
				88	347	23.4	355	0.484	
				143	330	37.4	853	0.277	
				77	231	30.2	361	0.457	
				72	361	14.7	306	0.983	
				72	355	14.8	318	0.971	
				105	424	16.6	518	0.828	
				100	433	19.1	588	0.883	
				120	438	18.7	628	0.924	

4. Results and discussion

4.1. Geochemistry and origin of Jurassic granitoids from Sanandaj to Sirjan

Jurassic intrusive rocks have a wide distribution along the Sanandaj-Sirjan Zone (Fig. 1). In this section, we focus on the geochemical affinities, origin and ages of Jurassic intrusive rocks with granitoid composition. Tables 1 and 2 list representative age, isotopic and geochemical data.

The SW Australia granitoids are generally classified as I-, A- and S-types, which refer to source rocks of fundamentally different origins (e.g., Whalen et al., 1987; Chappell & White, 2001; Frost et al., 2001; Clemens, 2003; Chappell et al., 2004, 2012; Grebennikov, 2014). By reconsidering an integrated collection of available major, rare earth and trace elements, and the isotopic data, we have

classified and interpreted the Jurassic granitoids of the Sanandaj-Sirjan Zone into three similar groups, characterised by S-type, I-type and A-type magmatic affinities.

4.1.1. S-type magmatism in Hamadan-Sirjan Zone

Samples from the Hamadan-Sirjan Zone exhibit a wide range of compositions from gabbroic diorite, diorite, granodiorite, quartz monzonite to granite (SiO_2 ~55–75 wt%; Na_2O+K_2O ~4–10 wt%; Fig. 2a). MORB- and chondrite-normalised patterns indicate that Jurassic granitoid samples from S-SaSZ are similarly enriched in LFSEs and HFSEs (i.e., Sr, K, Rb, Ba, Th, Nb, Ta) (Fig. 2b). Depletion of Ti (and P) (Fig. 2b) suggests ilmenite (+apatite) removal during partial melting or fractionation (Bonin, 2012). Enrichment in K and Th (Fig. 2b) reflects a crustal source or significant contamination (e.g., Soesoo, 2000; Fan et al., 2000). The samples exhibit LREE/HREE enrichment in the chondrite-normalised diagram with a nearly flat HREE profile, pronounced negative Eu anomaly (0.1–1), and $(La/Yb)_N$ ratios of ~5 to 15 (Fig. 2c). In the εNd_i versus $(^{87}Sr/^{86}Sr)_i$ diagram, samples plot in the field of continental crust with high ($^{87}Sr/^{86}Sr$) and low εNd_i (Fig. 3). The low $(Eu/Eu)_N$ ratios (Fig. 2d; Table 2) of these granitoids suggest oxygen-reducing conditions.

4.1.2. I- and A-type magmatism in the Sanandaj-Ghorveh Zone

From the Sanandaj to Ghorveh areas in the N- to C-SaSZ (i.e., Ghorveh, Mobarakabad, Shirvaneh, Ghalaylan, Bolbanabad, Varmaghan, Suffiabad), the gabbro-gabbroic diorite, monzonite, quartz monzonite and granite (Fig. 4a) have a wider compositional range of SiO_2 (~50–80 wt%) and Na_2O+K_2O (~4–11 wt%) than the samples from the Sanandaj-Ghorveh Zone. Based on SiO_2 *vs* K_2O classification diagram (Peccerillo & Taylor, 1976), they belong to calc-alkaline (e.g., Ghorveh diorites), high-K calc-alkaline (e.g., Ghalaylan, Mobarakabad) and shoshonite (e.g., Ghorveh monzonites, Varmaghan) magmatic series (Fig. 4b). In the MORB- and chondrite-normalised diagrams, they show LREE/HREE enrichment, flat HREE patterns, enrichment in LFSE and HFSE (i.e., Sr, K, Rb, Ba, Th, Ta, Nb) and depletion in Zr, Ti, P, Y and Yb (Figs. 4c, 4d, 4e, 4f). Granitoids from Ghorveh, Mobarakabad, Shirvaneh, and Suffiabad have a distinctive metaluminous affinity, while those from Varmaghan, Ghalaylan and Bolbanabad range from metaluminous to peraluminous.

4.1.2.a. I-type magmatism in the Sanandaj-Ghorveh Zone

On the Zr+Nb+Ce+Y *vs* FeO/MgO diagram (Whalen et al., 1987), the volcanic arc granites plot in the

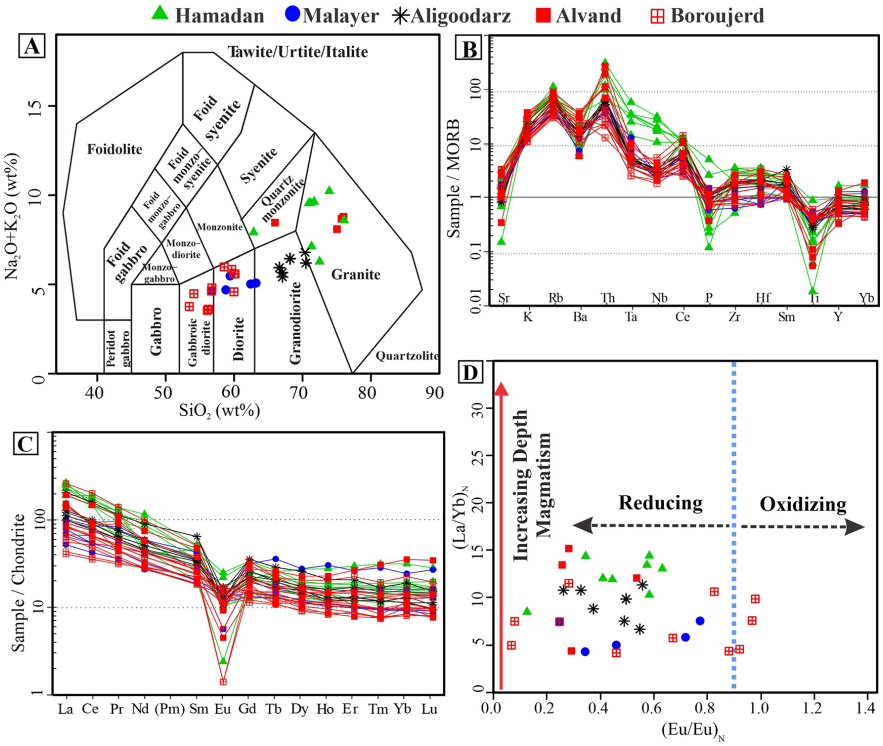

Fig. 2. Jurassic S-type rocks of the Sanandaj-Sirjan Zone. **A –** SiO_2 *vs* Na_2O+K_2O classification diagram (Middlemost, 1994); **B –** MORB-normalised diagram (normalisation values are from Pearce, 1983); **C –** Chondrite-normalised diagram (normalisation values are from Boynton, 1984); **D –** $(Eu/Eu)_N$ *vs* $(La/Yb)_N$ plot.

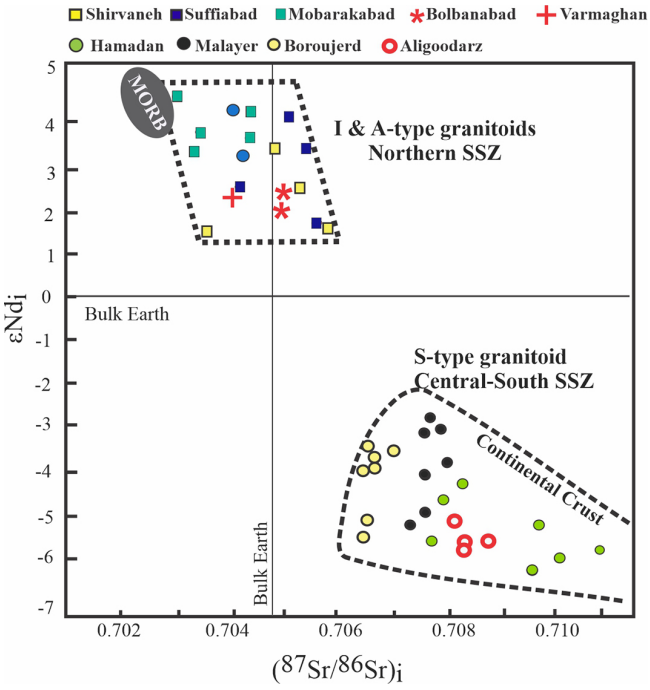

Fig. 3. Jurassic rocks of the Sanandaj-Sirjan Zone in $(^{87}Sr/^{86}Sr)_i$ *vs* εNd_i plot.

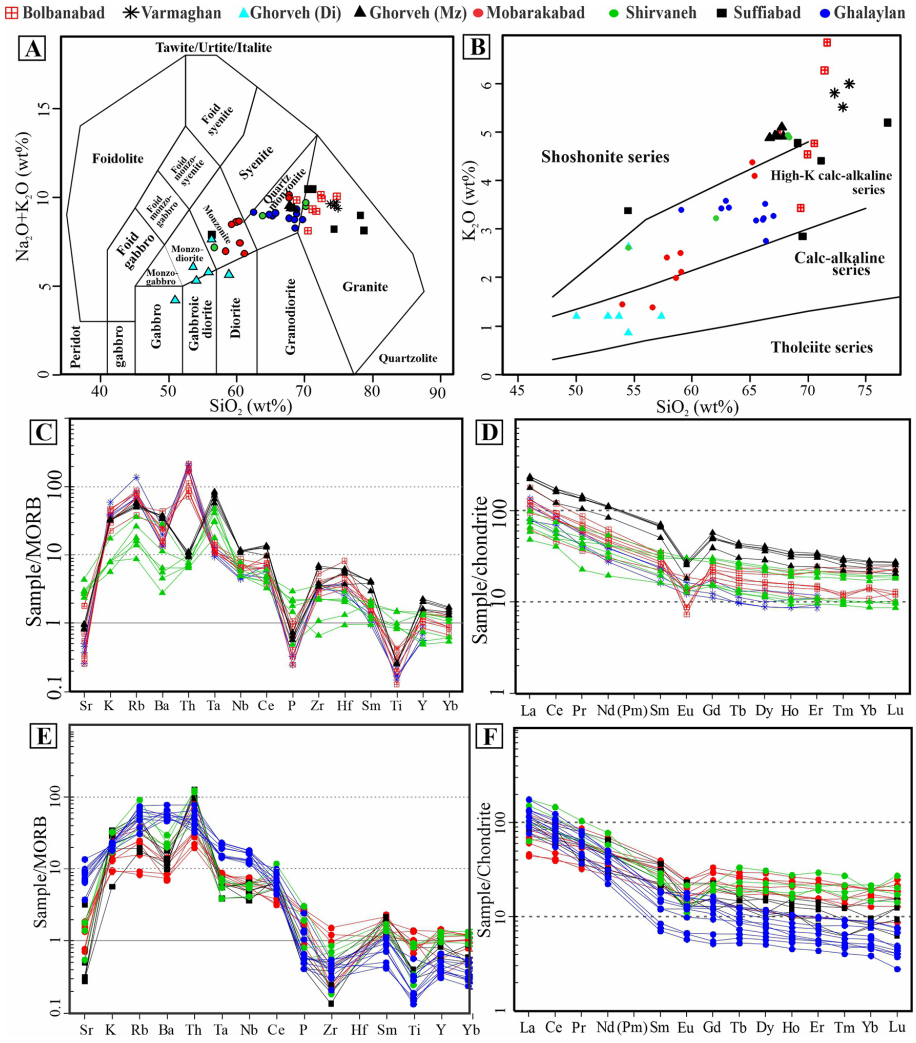

Fig. 4. Jurassic I- and A-type rocks from the northwest of the Sanandaj-Sirjan Zone. **A –** SiO_2 *vs* Na_2O+K_2O classification diagram (Middlemost, 1994); **B –** SiO_2 *vs* K_2O classification diagram (Peccerillo & Taylor, 1976); **C –** MORB-normalised diagram; **D –** chondrite-normalised diagram; **E –** MORB-normalised diagram; **F –** chondrite-normalised diagram. *Abbreviations*: Di: diorite; Mz: Monzonite; MORB and chondrite normalisation values are from Pearce (1983) and Boynton (1984), respectively.

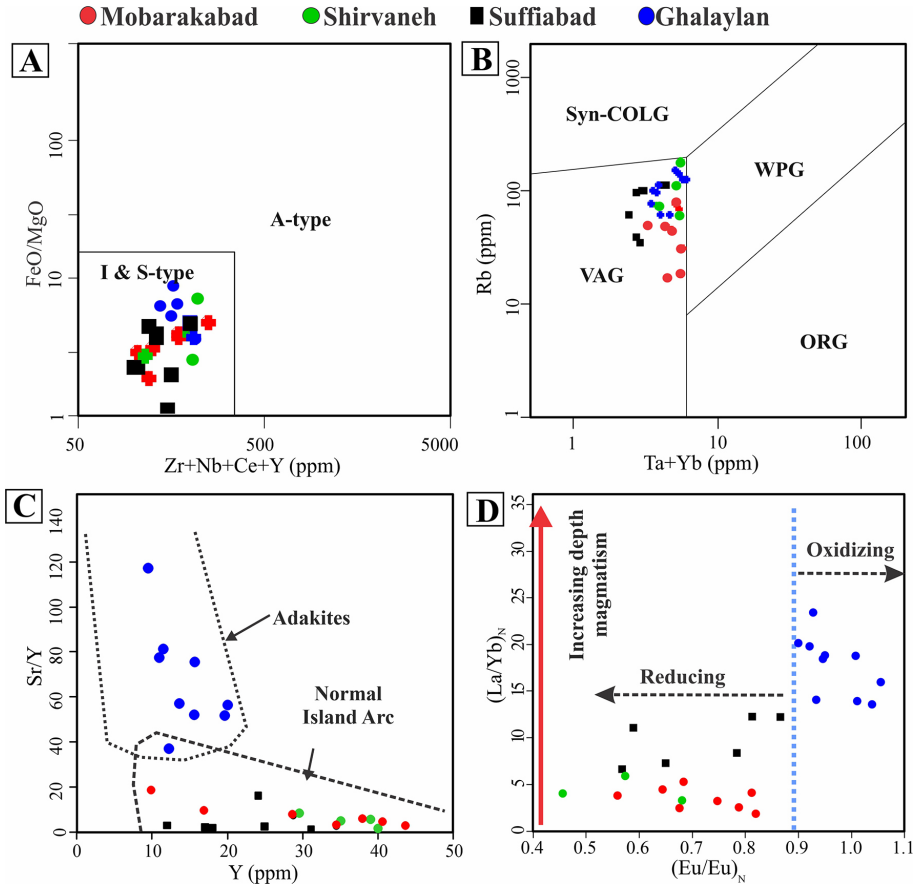

Fig. 5. Classification of Jurassic I-type rocks of the Sanandaj-Ghorveh Zone. **A –** Zr+Nb+Ce+Y *vs* FeO/MgO plot (Whalen et al., 1987); **B –** Ta+Yb *vs* Rb plot (Pearce et al., 1984); **C –** Y *vs* Sr/Y plot (after Defant & Drummond, 1990); **D –** $(Eu/Eu)_N$ *vs* $(La/Yb)_N$ plot *Abbreviations*: Syn-COLG: syn-collisional granites; VAG: volcanic arc granites; WPG: within-plate granites; ORG: oceanic ridge granites.

I-type granitoid field (Fig. 5a). The Ta+Yb *vs* Rb plot (Pearce et al., 1984) suggests that granitoids from Mobarakabad, Shirvaneh, Suffiabad and Ghalaylan areas are of volcanic arc origin (Fig. 5b). Elevated εNd_i (>1), with low $(^{87}Sr/^{86}Sr)_i$ of 0.703–0.706 (Fig. 3) support the classification of these rocks as calc-alkaline I-type, originating from partial melting of a garnet-bearing mantle source in a continental volcanic arc. Low Sr/Y ratios (<20) and high Y (> 10 ppm) contents of samples from the Mobarakabad, Shirvaneh and Suffiabad areas show a normal volcanic arc affinity; however, the high Sr/Y ratios (>40) and low Y values (<20 ppm) of Ghalaylan I-type granitoids resemble adakitic melts (Fig. 5c). As an indicator of the oxidation state of magma, $(Eu/Eu)_N$ ratios (Fig. 5d; Table 2) suggest oxygen-reducing (Mobarakabad, Shirvaneh and Suffiabad areas) to oxidising (Ghalaylan area) conditions.

4.1.2.b. A-type magmatism in the Sanandaj-Ghorveh Zone

The granitoids from the Varmaghan, Ghorveh and Bolbanabad areas are comparable with I-type rocks in high εNd_i (>1) and low $(^{87}Sr/^{86}Sr)_i$ of 0.703–0.706 (Fig. 3). However, they display known geochemical characteristics (e.g., Whalen et al., 1987) of A-type magmas including high Zr+Nb+Ce+Y contents (Fig. 6a) and Ga/Al ratios (Fig. 6b), low Sr/Y (Fig. 6c), $(Eu/Eu)_N$ ratio of 0.2–0.9 (that suggests a reduction state, except for few samples of Ghorveh diorite with $(Eu/Eu)_N$ of 1- 1.1) (Fig. 6d; Table 2), high Ta, Nb, Ce Zr, Hf concentrations and depletion in P, Sr and Ti (Fig. 4c) and HREE/LREE depletion (Fig. 4d).

Based on Loiselle & Wones (1979), A-type granites refer to magmas formed in an orogenic magmatic system; however, numerous occurrences of A-type granites generated in subduction-related extensional environments (Wu et al., 2002; Chen & Jahn, 2004; Mortimer et al., 2006; Zhao et al., 2008; Ahankoub et al., 2013). Jurassic igneous rocks are known to be the result of the formation of a window within the subducting Neo-Tethys slab, a process that caused the partial melting of overlying continental lithospheric material (e.g., Yang et al.,

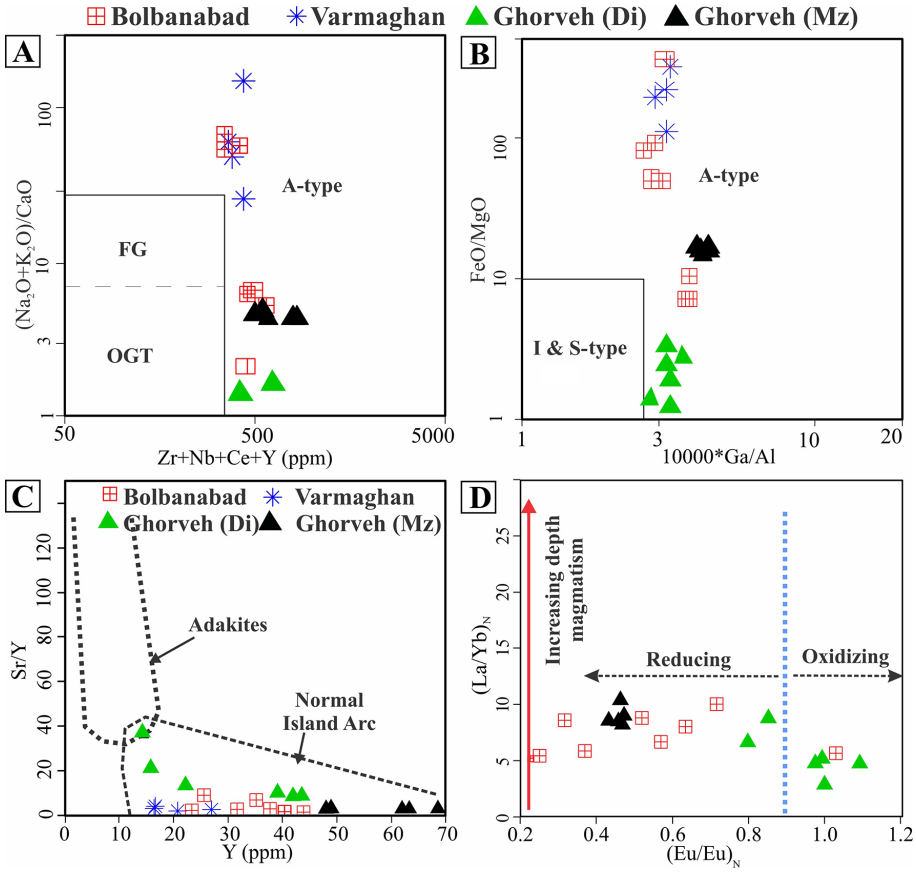

Fig. 6. Classification of Jurassic A-type rocks of the Sanandaj-Ghorveh Zone. **A –** 10000Ga/Al *vs* FeO/MgO (Whalen et al., 1987); **B –** Zr+Nb+Ce+Y *vs* FeO/MgO plot (Whalen et al., 1987); **C –** $(Eu/Eu)_N$ *vs* $(La/Yb)_N$ plot. *Abbreviations*: Di: diorite; Mz: Monzonite; FG: fractionated felsic granites; OGT: unfractionated I-, S-and M-type granites.

2018; Zhang et al., 2018a). A few Jurassic intrusives, however, formed in a subduction-related continental rift (Azizi et al., 2020b), emplaced between the N-SaSZ in the late Palaeozoic (360 Ma, Azizi et al., 2017) and the C-SaSZ in Middle (166–163 Ma, Tavakoli et al., 2020) to Late Jurassic (154–146 Ma, Azizi et al., 2020a). Azizi & Stern (2019) indicated that the most intense rifting happened in the C-SaSZ.

To sum up the results, a comparison of compiled data for the Jurassic granitoids indicates the negative Eu anomaly decreasing from S-type to A-type and I-type granitoids of the SaSZ (Figs. 2c, 4d, and 4f). I-type granitoids are low in Zr, Ta, and Sm but high in Rb, Sr, and Ba (Fig. 4e); whereas S-types are slightly enriched in Th and Nb (Fig. 2b). The A-types are contrasted by higher Zr, and Hf and lower Sr concentrations (Fig. 4c). The S-types granites have relatively very low (negative) εNd_i values, but a large $(^{87}Sr/^{86}Sr)_i$ range from 0.708 to 0.765 (Fig. 3). The I-types exhibit positive initial Nd, but a more limited $(^{87}Sr/^{86}Sr)_i$ range from 0.704 to 0.706 (Fig. 3). The A-type granites have high $(^{87}Sr/^{86}Sr)_i$ ratios from 0.702 to 0.717, but low (negative) εNd_i values (Fig. 3).

4.2. Geophysical data

The tectonic setting, source of magma and condition of melting control magnetite and ilmenite granitoids. Based on magnetic properties, Ishihara (1977) classified granitoids into magnetite and ilmenite series. The magnetite series contains magnetite and shows magnetic susceptibility higher than 100×10^{-5} SI. The magnetite series are ascribed to I-type granitoids, which occur mainly in the subduction zone under oxidising conditions. In the ilmenite series, magnetic susceptibility is usually less than 50×10^{-5} SI. These rocks are supposed to have originated within the continental crust under reducing conditions. There is uncertainty in the interpretation of granitoids and magnetic content due to alteration because magnetite content and the magnetic susceptibility will change due to the alteration intensity of granitoids. The highest magnetic susceptibility values in Iran are related to the Cenozoic Urumieh-Dokhtar magmatic belt (Fig. 7a), where Cenozoic granitoids of magnetite series are exposed (e.g., Golestani et al., 2018; Raeisi et al., 2019; Kazemi et al., 2019, etc.). Based on the magnetic susceptibil-

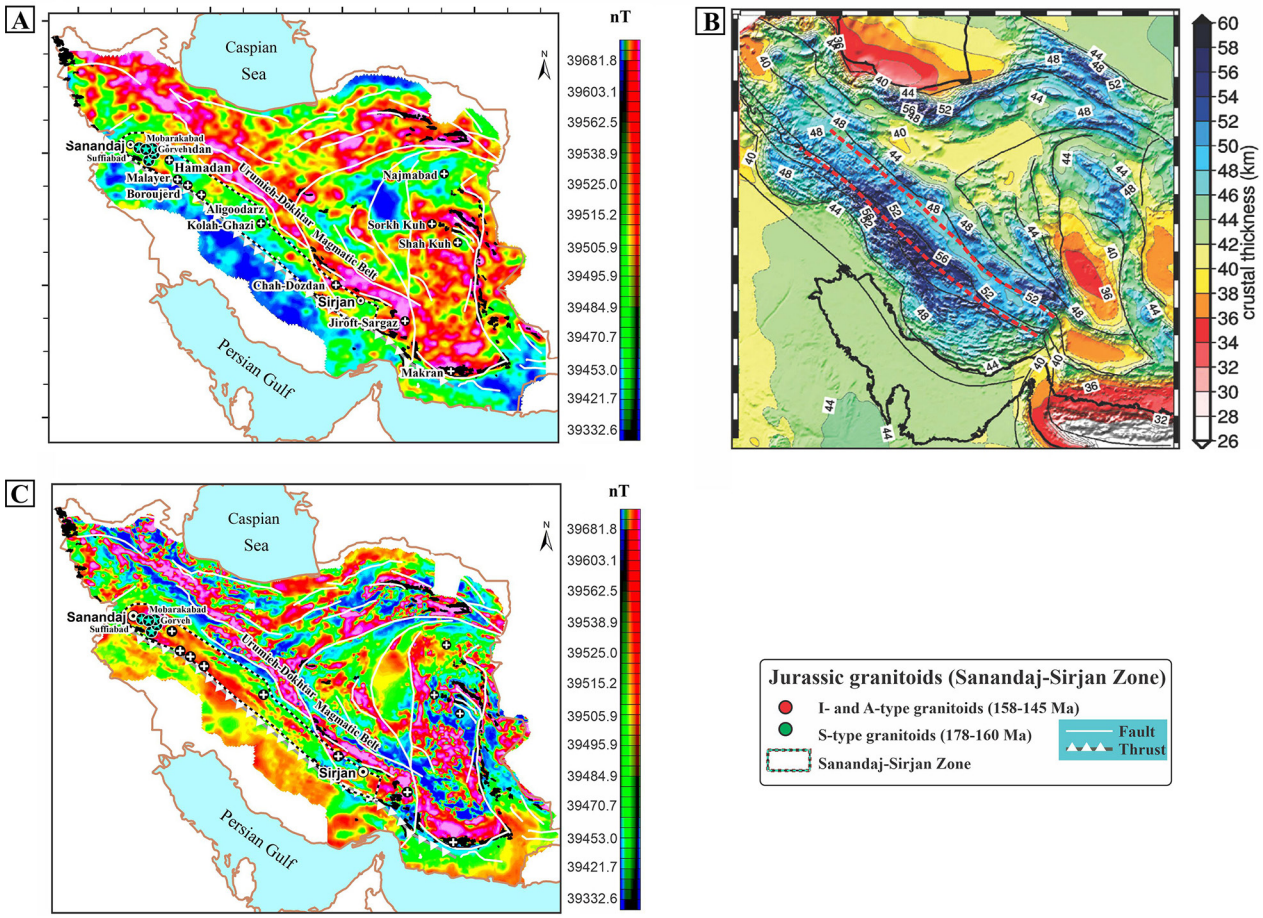

Fig. 7. Location of Jurassic granitoid rocks along the SaSZ. A – magnetic susceptibility map of Iran (from Teknik & Ghods, 2017)); B – Crustal thicknesses in structural zones of Iran determined by combining elevation and geoid data (Jiménez-Munt et al., 2012); C – Location of Jurassic granitoid rocks along the SaSZ plotted on an aeromagnetic map of Iran (rotation to pole RTP) (aeromagnetic map from Teknik & Ghods, 2017).

ity map (Teknik & Ghods, 2017), S-type Jurassic granitoids of SaSZ (Hamdan, Malayer, Boroujerd, Aligoodarz, Kolah Ghazi and Chah Dozdan) show low magnetic susceptibility (<100 × 10^{-5}; Fig. 7a); therefore, they belong to the ilmenite series. In contrast, granitoids from the Ghorveh, Mobarakabad, Shirvaneh, Ghalaylan, Bolbanabad, Varmaghan and Suffiabad areas have high magnetic susceptibility (>100 × 10^{-5}; Fig. 7a), similar to I-type granitoids of the magnetite series (oxidised type granitoid).

In addition, the geophysical data have revealed that the continental crust has the highest thickness of 52–56 km between Hamadan to Sirjan (Jiménez-Munt et al., 2012) (Fig. 7b). It can be related to the continental collision during the Cimmerian orogeny between 178 and 160 million years ago.

The western boundary of the Sanandaj-Sirjan Zone is defined by the major Zagros thrust fault (Fig. 1). The magnetic anomalies along the thrust and to the west of the major thrust fault are very important to take into account. The aeromagnetic map of Teknik & Ghods (2017) (Fig. 7c) shows there are some igneous rocks (e.g., ophiolitic rocks) under the thrust areas. Thus, the movement of the thrust covered the igneous rocks that could be the remnants of Tethyan ophiolites and Late Triassic-Early Jurassic volcanic arcs.

4.3. Geochronological data

In addition to different geochemistry and origin, Jurassic S-type granitoids from C- to S-SaSZ typically show ages older than Middle Jurassic (including plutonic rocks of W–S Hamedan (164–165 Ma; Chiu et al., 2013), Malayer (162–184 Ma; Ahadnejad et al., 2011), Boroujerd (170–172 Ma; Khalaji et al., 2007), Aligoodarz (167–170 Ma; Zhang et al., 2018b), Kolah Ghazi (167–175 Ma; Bayati et al., 2017), Qhory (170–173 Ma; Yang et al., 2018) and Jiroft-Sargaz (175 Ma; Chiu et al., 2013); Table 1), while the I- and A-type granitoids of the Sanandaj

region and Ghorveh Plutonic Complex (Table 1; Figs. 8 and 9) in the west of Ghorveh city (N-SaSZ) reveal younger ages ranging between 158 and 147 Ma (including plutonic rocks of Mobarakabad (147, 148 Ma; Zhang et al., 2018b), Taghiabad-Kangareh (155, 150 Ma; Azizi et al., 2015a), Ghalaylan (156, 158 Ma; Azizi et al., 2015b), South Ghorveh (146, 150 Ma; Zhang et al., 2018a), Bolbanabad (146 Ma; Zhang et al., 2018a), Suffiabad (148, 145 Ma; Azizi et al., 2011), Shirvaneh (146, 152, 154 Ma; Azizi et al., 2020a) and Ghorveh-Dehgolan (150 Ma; Yajam et al., 2015); Fig. 8).

Accordingly, we divide the SaSZ into the (1) Sanandaj-Ghorve and (2) Hamadan-Sirjan tectonomagmatic zones, because of two contrasting Jurassic magmatisms with different ages and origins. The Sanandaj-Ghorve Zone comprises Jurassic granitoids that occur between Sanandaj and Ghorveh (i.e., Ghorveh, Mobarakabad, Shirvaneh, Ghalaylan, Bolbanabad, Varmaghan and Suffiabad areas; Fig. 9). Jurassic granitoids of the Hamadan-Sirjan Zone in the C- to S-SaSZ, are spatially distributed from Ghorveh to W-S Hamedan, Alvand, Malayer, Boroujerd and Aligoodarz areas (Fig. 9).

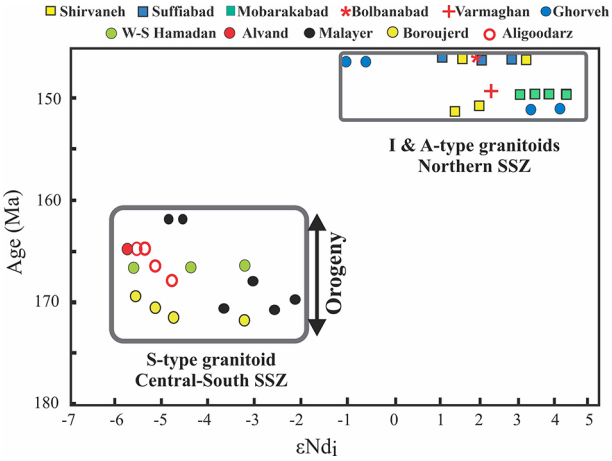

Fig. 8. Jurassic intrusive rocks of the Sanandaj-Sirjan Zone in εNd_i *vs* age (in Ma) plot.

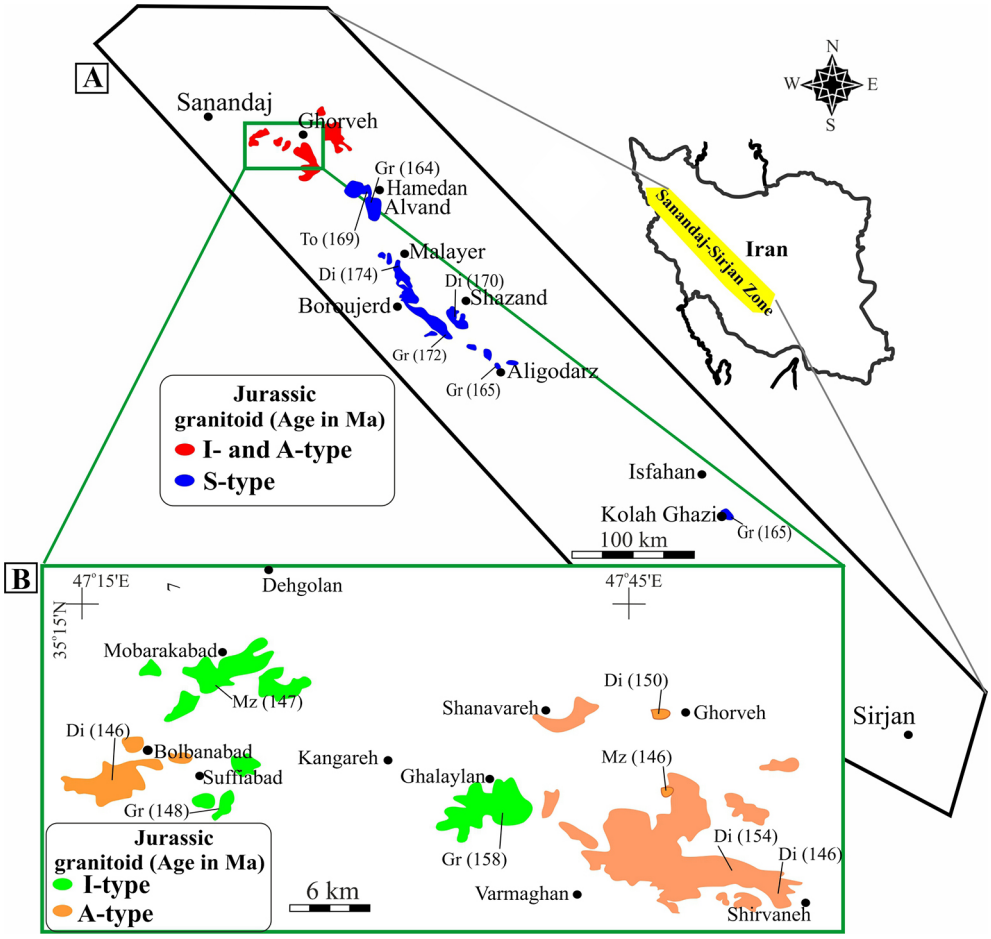

Fig. 9. Distribution of Jurassic intrusive rocks along the Sanandaj-Sirjan Zone (Mobarakabad (147/148 Ma; Zhang et al., 2018a), Taghiabad-Kangareh (155-150 Ma; Azizi et al., 2015a), Ghalaylan (156-158 Ma; Azizi et al., 2015b), South Ghorveh (150-146 Ma; Zhang et al., 2018a), Bolbanabad (146 Ma; Zhang et al., 2018a), Suffiabad (148-145 Ma; Azizi et al., 2011), Shirvaneh (154-146 Ma; Azizi et al., 2020a) and Ghorveh-Dehgolan (150 Ma; Yajam et al., 2015).

4.4. Tectonomagmatic setting

Mesozoic to Cenozoic magmatic and metamorphic events in the SaSZ are summarised in Figure 10. The subduction of the Neo-Tethys oceanic crust beneath the SaSZ resulted in the complete closure of the Palaeo-Tethys Ocean in the early Late Triassic (Mehdipour Ghazi & Moazzen, 2015). Then, an orogenic episode (Cimmerian orogeny) affected the Sanandaj–Sirjan Zone in the Early to Middle Jurassic (e.g., Fergusson et al., 2016). This event is recorded by deformation and metamorphism under greenschist facies condition (Sheikholeslami, 2015) and formation of slate and phyllite.

Between 178 and 160 Ma, the S-type granitoids in the Hamadan-Sirjan Zone (i.e., W-S Hamedan, Malayer, Aligoodarz and Boroujerd; Table 1) formed as a result of closure of the Palaeo-Tethys and subsequent continental collision during the Cimmerian orogeny in the southwestern margins of the Sanandaj-Sirjan Zone (e.g., Fergusson et al., 2016). Contact metamorphism occurred during the emplacement of S-type granitoids in the schists of the Hamadan-Sirjan Zone (i.e., W-S Hamedan, Malayer, Aligoodarz and Boroujerd).

About 15 million years later (~158–145 Ma), an active continental margin developed from the Sanandaj-Ghorve Zone (e.g., Mohajjel & Fergusson, 2014; Fergusson et al., 2016). In the Sanandaj-Ghorve Zone, the extensional (e.g., Zhang et al., 2018a) and I-type (e.g., Azizi et al., 2011, 2013, 2015b, 2020a) magmatism developed in the Sanandaj to Ghorveh regions (i.e., Ghorveh, Mobarakabad, Suffiabad, Shirvaneh, Ghalaylan, Varmaghan and Bolbanabad areas) (Table 1). The marble and schist in the Ghalaylan complex (145–144 Ma) recorded a metamorphic event in the lower greenschist facies (Azizi et al., 2018), while the Ar-Ar ages marked a Cenozoic, low-grade metamorphic overprint during the Alpine orogeny (e.g., Shakerardakani et al., 2015; Monfaredi et al., 2020).

In the Hamadan-Sirjan Zone, intrusive rocks (W-S Hamedan, Malayer, Boroujerd, Aligoodarz, Kolah Ghazi and Chah Dozdan) that were emplaced during the Cimmerian orogeny (178 to 160 Ma) along the SaSZ, were not related to a volcanic arc subduction zone, but to a continental collision setting. This is documented by geological evidence as follows:

a) during the period of 178 to 160 Ma, there was no volcanism. All these intrusive rocks form a batholith, emplaced at depths in excess of 4 km, thus they are not sub-volcanic rocks. Detrital sedimentary rocks formed during erosion after the emplacement of plutonic rocks;
b) the Cimmerian orogeny caused regional metamorphism along the SaSZ (Fergusson et al., 2016; Monfaredi et al., 2020). For example, there are regional high-grade metamorphic rocks of Early to mid-Jurassic age (Baharifar et al., 2004). Thus, all granitoids which were emplaced during the Cimmerian orogeny were syn-collisional;
c) the elevated thickness of continental crust in this region (Fig. 7b), the S-type magmatism of the

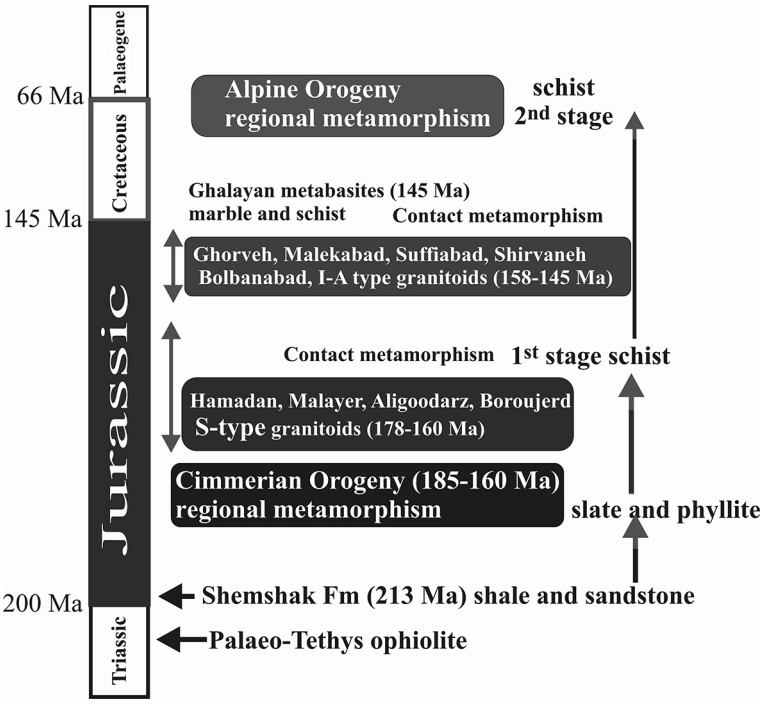

Fig. 10. Metamorphic events in the Sanandaj-Sirjan Zone.

Hamadan-Sirjan Zone, as well as the regional high-grade metamorphism of Jurassic age occurred in a continental collision regime between 178 and 160 Ma as a result of the Cimmerian orogeny.

A continental collision setting in the Hamadan-Sirjan Zone in 178–160 Ma and then a subduction-related extensional environment in the Sanandaj-Ghorve Zone in 158–145 Ma are in accord with a heterogenic subcontinental lithospheric mantle, likely caused by oblique subduction or slab break-off.

4.5. Cimmerian S-type granites in the Hamadan-Sirjan Zone and east of Iran

Previous concepts on the origin and tectonomagmatic setting of C- to S-SaSZ Jurassic granitoids of 178–160 Ma in the Hamadan to Sirjan Zone (i.e., west to South Hamedan (W-S Hamedan), Alvand, Malayer, Boroujerd, Aligoodarz) are (1) metaluminous I-type granites formed in a magmatic arc of an Andean subduction system (Khalaji et al., 2007; Tahmasbi et al., 2010; Ahadnejad et al., 2011; Esna-Ashari et al., 2012), (2) subduction-related extensional basin (Shahbazi et al., 2010), (3) continental crust melting by roll-back of a Neo-Tethys oceanic crust (Zhang et al., 2018b) and (4) subduction-related, S-type granites (Bayati et al., 2017). However, contrary to previous studies, a re-evaluation of the geological (e.g., absence of volcanic arc and volcanic rocks, formation of large-scale (batholith) granitoids at depths >4 km, regional metamorphism at greenschist (and amphibolite) facies during the Cimmerian orogeny), geophysical (e.g., continental crust thickening (56–52 km), magnetic susceptibility $<100 \times 10^{-5}$ (ilmenite series)) and geochemical (e.g., low $(Eu/Eu)_N$ and reducing conditions (Fig. 2d), negative εNdi and elevated $(^{87}Sr/^{86}Sr)_i$ >0.707), see Fig. 3) characteristics of granitoids in the SaSZ indicates that the granitoids originated from anatectic S-type melts formed by partial melting of lower continental crust in a continental margin during the Cimmerian orogeny.

In the east of Iran, similar outcrops of S-type granites (ilmenite series) from the Najmabad (161.85 Ma, Sr_i=0.7091, εNd_t=-6.51; Moradi Noghondar et al., 2011) and Sorkh Kuh regions (165 Ma, Sr_i=0.707; Tarkian et al., 1983) to Shah Kuh region (165 Ma, Sr_i=0.7065, εNd_t=-2.5; Esmaeily et al., 2005) (Fig. 1) all have the characteristics of the Hamadan-Sirjan Zone granitoids in the time range of 178–160 Ma. The Jurassic (163–166 Ma) batholiths of eastern Iran mainly intruded into pre-Jurassic slates (e.g., Deh Salam metamorphic complex; Esmaeily et al., 2005) during the Cimmerian orogeny. Based on low magnetic susceptibility ($<100 \times 10^{-5}$), they belong to the ilmenite series. Neither volcanic rocks nor volcanic arc formed in this time. The Rb-Sr and Sm-Nd isotope data (e.g., Tarkian et al., 1983; Esmaeily et al., 2005; Moradi Noghondar et al., 2011) indicate that the magma originated from a continental crust. These geochemical and geophysical features confirm the simultaneous continental collision magmatism in the Hamadan-Sirjan Zone and east of Iran during the Cimmerian orogeny.

5. Conclusions

A comparison of compiled geochemical and geochronological data and contrasting Jurassic geological events along the SaSZ suggests a division of the Sanandaj-Sirjan Zone into two tectonomagmatic zones on account of a heterogenic subcontinental lithospheric mantle: the Hamadan-Sirjan and Sanandaj-Ghorveh zones.

(1) In the Hamadan-Sirjan Zone (i.e., Boroujerd, Malayer, Aligoodarz, W-S Hamedan and Alvand regions), Jurassic (178–160 Ma) granites with εNd_i <-2, $(^{87}Sr/^{86}Sr)_i$ >0.706, and low magnetic susceptibility ($<100 \times 10^{-5}$) are classified as S-type granitoids belonging to the ilmenite series that formed by partial melting of a lower continental crust under reducing conditions ($(Eu/Eu)_N$ =0.4–0.8). These granitoids were formed during the Cimmerian orogeny due to continental collision. Their emplacement within slate resulted in regional metamorphism in the C- to S-SaSZ. Important geological (e.g., the absence of volcanism during 178 to 160 Ma, emplacement depth of intrusive rocks (>4 km), occurrence as large-scale intrusions, and the regional high-grade metamorphism), isotopic geochemical (e.g., low $(Eu/Eu)_N$ and reducing conditions, negative εNdi and elevated $(^{87}Sr/^{86}Sr)_i$ >0.707) and geophysical (e.g., the elevated thickness of continental crust (56–52 km), magnetic susceptibility $<100 \times 10^{-5}$ (ilmenite series)) evidence show that these rocks were associated with a *continental collision setting* and not related to volcanic arc subduction zone.

(2) In the Sanandaj-Ghorveh Zone (i.e., Ghorveh, Mobarakabad, Shirvaneh, Ghalaylan, Bolbanabad, Varmaghan and Suffiabad regions) the Jurassic (158–145 Ma) high-K calc-alkaline granitoids revealed two distinct origins:

(a) I-type granitoids from the Mobarakabad, Shirvaneh and Suffiabad areas with εNd_i>1, $(^{87}Sr/^{86}Sr)_i$ of 0.703–0.706, and high magnet-

ic susceptibility (>100 × 10^{-5}) occurred in an arc-related environment with an oxidising condition ($(Eu/Eu)_N$ = 0.9–1.2) from partial melting of a garnet-bearing mantle source in a continental collision zone;

(b) A-type granitoids from the Varmaghan, Ghorveh and Bolbanabad areas with εNd_i>1 and $(^{87}Sr/^{86}Sr)_i$ of 0.703–0.706, show diagnostic features of a subduction-related extensional environment. Despite the occurrence of some A-type rocks in the Sanandaj-Ghorveh region, I-type rocks are more frequent than any other intrusive in this region.

Acknowledgements

The authors wish to thank Dr Abdolreza Ghods for discussions regarding the aeromagnetic and magnetic susceptibility maps of Iran.

References

Abdulzahra, I.K., Hadi, A., Asahara, Y., Azizi, H. & Yamamoto, K., 2018. Petrogenesis and geochronology of Mishao peraluminous I-type granites, Shalair valley area, NE Iraq. *Chemie der Erde* 78, 215–227.

Agard, P., Omrani, J., Jolivet, L. & Mouthereau, F., 2005. Convergence history across Zagros (Iran): constraints from collisional and earlier deformation. *International Journal of Earth Sciences* 94, 401–419.

Agard, P., Omrani, J., Jolivet, L., Whitechurch, H., Vrielynck, B., Spakman, W., Monié, P., Meyer, B. & Wortel, R., 2011. Zagros orogeny: A subduction-dominated process. *Geological Magazine* 148, 692–725.

Ahadnejad, V., Valizadeh, M., Deevsalar, R. & Rezaei-kahkhaei, M., 2011. Age and geotectonic position of the Malayer granitoids: Implication for plutonism in the Sanandaj-Sirjan Zone, W Iran. *Neues Jahrbuch für Geologie und Paläontologie – Abhandlungen* 261, 61–75.

Ahankoub, M., Jahangiri, A., Asahara, Y. & Moayyed, M., 2013. Petrochemical and Sr-Nd isotope investigations of A-type granites in the east of Misho, NW Iran. *Arabian Journal of Geosciences* 6, 4833–4849.

Ajirlu, M.S., Moazzen, M. & Hajialioghli, R., 2016. Tectonic evolution of the Zagros Orogen in the realm of the Neotethys between the Central Iran and Arabian Plates: An ophiolite perspective. *Central European Geology* 59, 1–27.

Alavi, M., 1994. Tectonics of the Zagros orogenic belt of Iran: new data and interpretations. *Tectonophysics* 229, 211–238.

Alavi, M., 2007. Structures of the Zagros fold-thrust belt in Iran. *American Journal of Science* 307, 1064–1095.

Azizi, H. & Asahara, Y., 2013. Juvenile granite in the Sanandaj – Sirjan Zone, NW Iran: Late Jurassic – Early Cretaceous. *International Geology Review* 55, 1523–1540.

Azizi, H. & Jahangiri, A., 2008. Cretaceous subduction-related volcanism in the northern. *Journal of Geodynamics* 45, 178–190.

Azizi, H. & Stern, R.J., 2019. Jurassic igneous rocks of the central Sanandaj–Sirjan Zone (Iran) mark a propagating continental rift, not a magmatic arc. *Terra Nova* 31, 415–423.

Azizi, H., Asahara, Y., Mehrabi, B. & Lin, S., 2011. Geochronological and geochemical constraints on the petrogenesis of high-K granite from the Suffi Abad area, Sanandaj-Sirjan Zone, NW Iran. *Chemie der Erde – Geochemistry* 71, 363–376.

Azizi, H., Asahara, Y., Minami, M. & Anma, R., 2020a. Sequential magma injection with a wide range of mixing and mingling in Late Jurassic plutons, southern Ghorveh, western Iran. *Journal of Asian Earth Sciences* 200, 104469.

Azizi, H., Kazemi, T. & Asahara, Y., 2017. A-type granitoid in Hasansalaran complex, northwestern Iran: Evidence for extensional tectonic regime in northern Gondwana in the Late Paleozoic. *Journal of Geodynamics* 108, 56–72.

Azizi, H., Lucci, F., Stern, R.J., Hasannejad, S. & Asahara, Y., 2018. The Late Jurassic Panjeh submarine volcano in the northern Sanandaj- Sirjan Zone, northwest Iran: Mantle plume or active margin? *Lithos* 308–309, 364–380.

Azizi, H., Najari, M., Asahara, Y., Catlos, E.J., Shimizu, M. & Yamamoto, K., 2015a. U-Pb zircon ages and geochemistry of Kangareh and Taghiabad mafic bodies in northern Sanandaj–Sirjan Zone, Iran: Evidence for intra-oceanic arc and back-arc tectonic regime in Late Jurassic. *Tectonophysics* 660, 47–64.

Azizi, H., Nouri, F., Stern, R.J., Azizi, M., Lucci, F., Asahara, Y., Zarinkoub, M.H. & Chung, S.L., 2020b, New evidence for Jurassic continental rifting in the northern Sanandaj Sirjan Zone, western Iran: the Ghalaylan seamount, southwest Ghorveh. *International Geology Review* 1–23.

Azizi, H., Zanjefili-Beiranvand, M. & Asahara, Y., 2015b. Zircon U–Pb ages and petrogenesis of a tonalite–trondhjemite–granodiorite (TTG) complex in the northern Sanandaj–Sirjan zone, northwest Iran: Evidence for Late Jurassic arc–continent collision. *Lithos* 216–217, 178–195.

Badr, A., Davoudian, A., Shabanian, N., Azizi, H., Asahara, Y., Neubauer, F., Dong, Y. & Yamamoto, K., 2018. A- and I-type metagranites from the North Shahrekord Metamorphic Complex, Iran: Evidence for Early Paleozoic post-collisional magmatism. *Lithos* 300–301, 86–104.

Baharifar, A., Moinevaziri, H., Bellon, H. & Piqué, A., 2004. The crystalline complexes of Hamadan (Sanandaj – Sirjan zone, western Iran): metasedimentary Mesozoic sequences affected by Late Cretaceous tectono-metamorphic and plutonic events. *Comptes Rendus Geoscience* 336, 1443–1452.

Bayati, M., Esmaeily, D., Maghdour-Mashhour, R., Li, X. & Stern, R.J., 2017. Geochemistry and petrogenesis of Kolah-Ghazi granitoids of Iran: Insights into the Ju-

rassic Sanandaj-Sirjan magmatic arc. *Chemie der Erde – Geochemistry* 77, 281–302.

Berberian, M. & King, G.C.P., 1981. Towards a paleogeography and tectonic evolution of Iran. *Canadian Journal of Earth Sciences* 18, 210–265.

Bonin, B., 2012. Extra-terrestrial igneous granites and related rocks: A review of their occurrence and petrogenesis. *Lithos* 153, 3–24.

Boynton, W., 1984. Cosmochemistry of rare earth elements: meteorite studies [In:] Henderson, P. (Ed): *Rare earth element geochemistry*. Elsevier, Amsterdam, 63–114.

Chappell, B.W., 2004. Granites of the Lachlan Fold Belt. The Ishihara Symposium. *Granites and Associated Metallogenesis* 39–41.

Chappell, B.W. & White, A.J.R., 2001. Two contrasting granite types: 25 years later. Australian *Journal of Earth Sciences* 48, 489–499.

Chappell, B.W., Bryant, C.J. & Wyborn, D., 2012. Peraluminous I-type granites. *Lithos* 153, 142–153.

Chappell, B.W., White, A.J.R., Williams, I.S. & Wyborn, D., 2004. Low- and high-temperature granites. *Transactions of the Royal Society of Edinburgh, Earth Sciences* 95, 125–140.

Chen, B. & Jahn, B., 2004. Genesis of post-collisional granitoids and basement nature of the Junggar Terrane, NW China: Nd–Sr isotope and trace element evidence. *Journal of Asian Earth Sciences* 23, 691–703.

Chiu, H.Y., Chung, S.L., Zarrinkoub, M.H., Mohammadi, S.S., Khatib, M.M. & Iizuka, Y., 2013. Zircon U-Pb age constraints from Iran on the magmatic evolution related to Neotethyan subduction and Zagros orogeny. *Lithos* 162–163, 70–87.

Clemens, J.D., 2003. S-type granitic magmas – petrogenetic issues, models and evidence. *Earth-Science Reviews* 61, 1–18.

Clemens, J.D. & Stevens G., 2012. What controls chemical variation in granitic magmas ? *Lithos* 134–135, 317–29.

Clemens, J.D., Stevens, G. & Farina, F., 2011. The enigmatic sources of I-type granites: The peritectic connexion. *Lithos* 126, 174–181.

Daneshvar, N., Maanijou, M., Azizi, H. & Asahara, Y., 2019. Petrogenesis and geodynamic implications of an Ediacaran (550 Ma) granite complex (metagranites), southwestern Saqqez, northwest Iran. *Journal of Geodynamics* 132, 101669.

Deevsalar, R., Shinjo, R., Ghaderi, M., Murata, M., Hoskin, P.W.O., Oshiro, S., Wang, K.L., Lee, H.Y. & Neill, I., 2018. Mesozoic–Cenozoic mafic magmatism in Sanandaj–Sirjan Zone, Zagros Orogen (Western Iran): Geochemical and isotopic inferences from Middle Jurassic and Late Eocene gabbros. *Lithos* 284–285, 588–607.

Defant, M. & Drummond, M., 1990. Derivation of some modern arc magmas by melting of young subducted lithosphere. *Nature* 347, 662–665.

Ellwood, B.B. & Wenner, D.B., 1981. Correlation of magnetitic susceptibility with $^{18}O/^{16}O$ data in late orogenic granites of the southern Appalachian Piedmont. *Earth and Planetary Science Letters* 54, 200–202.

Esmaeily, D., Nedelec, A., Valizadeh, M., Moore, F. & Cotton, J., 2005. Petrology of the Jurassic Shah-Kuh granite (eastern Iran), with reference to tin mineralization. *Journal of Asian Earth Science* 25, 961–980.

Esna-Ashari, A., Tiepolo, M., Valizadeh, M., Hassanzadeh, J. & Sepahi, A., 2012. Geochemistry and zircon U–Pb geochronology of Aligoodarz granitoid complex, Sanandaj-Sirjan Zone, Iran. *Journal of Asian Earth Sciences* 43, 11–22.

Fan W.M., Zhang H.F., Baker J., Jarvis K.E., Mason P.R.D. & Menzies M.A., 2000. On and off the North China Craton: Where is the Archaean keel? *Journal of Petrology* 41, 933–950.

Fergusson, C.L., Nutman, A.P., Mohajjel, M. & Bennett, V.C., 2016. The Sanandaj – Sirjan Zone in the Neo-Tethyan suture, western Iran: Zircon U – Pb evidence of late Palaeozoic rifting of northern Gondwana and mid-Jurassic orogenesis. *Gondwana Research* 40, 43–57.

Frost, B.R., Barnes, C.G., Collins, W.J., Arculus, R.J., Ellis, D.J. & Frost, C.D., 2001. A geochemical classification for granitic rocks. *Journal of Petrology* 42, 2033–2048.

Ghasemi, A. & Talbot, C.J., 2006. A new tectonic scenario for the Sanandaj-Sirjan Zone (Iran). *Journal of Asian Earth Sciences* 26, 683–693.

Gill R., 2010. *Igneous Rocks and Processes: A Practical Guide*. John Wiley & Sons Ltd, UK, 428 pp.

Golestani, M., Karimpour, M.H., Malekzadeh Shafaroudi, A. & Hidarian Shahri, M.R., 2018. Geochemistry, U-Pb geochronology and Sr-Nd isotopes of the Neogene igneous rocks, at the Iju porphyry copper deposit, NW Shahr-e-Babak, Iran. *Ore Geology Reviews* 93, 290–307.

Grebennikov, A. V, 2014. A-type granites and related rocks: Petrogenesis and classification. *Russian Geology and Geophysics* 55, 1353–1366.

Hassanzadeh, J., Stockli, D.F., Horton, B.K., Axen, G.J., Stockli, L.D., Grove, M., Schmitt, A.K. & Walker, J.D., 2008. U-Pb zircon geochronology of late Neoproterozoic-Early Cambrian granitoids in Iran. Implications for paleogeography, magmatism, and exhumation history of Iranian basement. *Tectonophysics* 451, 71–96.

Hemmati, O., Tabatabaei Manesh, S.M. & Nadimi, A.R., 2018. Deformation Mechanisms of Darreh Sary Metapelites, Sanandaj□Sirjan Zone, Iran. *Geotectonics* 52, 281–296.

Homke, S., Vergés, J., Beek, P., Fernández, M., Saura, E., Barbero, L., Badics, B. & Labrin, E., 2010. Insights in the exhumation history of the NW Zagros from bedrock and detrital apatite fission-track analysis: evidence for a long-lived orogeny. *Basin Research* 22, 659–680.

Hunziker, D., Burg, J., Bouilhol, P. & Quadt, A., 2015. Jurassic rifting at the Eurasian Tethys margin: Geochemical and geochronological constraints from granitoids of North Makran, southeastern Iran. *Tectonics* 34, 571–593.

Ishihara, S., 1977. The magnetite-series and ilmenite-series granitic rocks. *Mining Geology* 27, 293–305.

Jamshidibadr, M., Collins, A.S., Masoudi, F., Cox, G. & Mohajjel, M., 2013. The U-Pb age, geochemistry and tectonic significance of granitoids in the Soursat Com-

plex, Northwest Iran. *Turkish Journal of Earth Sciences* 22, 1–31.

Jiménez-Munt, I., Fernàndez, M., Saura, E., Vergés, J. & Garcia-Castellanos, D., 2012, 3-D lithospheric structure and regional/residual Bouguer anomalies in the Arabia–Eurasia collision (Iran). *Geophysical Journal International* 190, 1311–1324.

Karimpour, M.H., Shirdashtzadeh, N. & Sadeghi, M., 2021. Granitoids of Sanandaj-Sirjan Zone that are concurrent with Cimmerian Orogeny (178–160 Ma) belong to ilmenite series (S-type): investigation of reason for lacking the porphyry tin mineralization. [In persian with English summary] *Journal of Economic Geology* 13, 1–28.

Kazemi, K., Kananian, A., Xiao Y. & Sarjoughian, F., 2019. Petrogenesis of Middle-Eocene granitoids and their mafic microgranular enclaves in central Urmia-Dokhtar Magmatic Arc (Iran): Evidence for interaction between felsic and mafic magmas. *Geoscience Frontiers* 10, 705–723.

Khalaji, A.A., Esmaeily, D. & Valizadeh, M.V, 2007. Petrology and geochemistry of the granitoid complex of Boroujerd, Sanandaj-Sirjan Zone, Western Iran. *Journal of Asian Earth Sciences* 29, 859–877.

Le Garzic, E., Vergés, J., Sapin, F., Saura, E., Meresse, F. & Ringenbach, J.C., 2019. Evolution of the NW Zagros Fold-and-Thrust Belt in Kurdistan Region of Iraq from balanced and restored crustal-scale sections and forward modeling. *Journal of Structural Geology* 124, 51–69.

Loiselle, M. & Wones, D., 1979. Characteristics and origin of anorogenic granites. *Society of America, Abstract with Programs* 11, 468.

Mahmoudi, S., Corfu, F., Masoudi, F., Mehrabi, B. & Mohajjel, M., 2011. U-Pb dating and emplacement history of granitoid plutons in the northern Sanandaj-Sirjan Zone, Iran. *Journal of Asian Earth Sciences* 41, 238–249.

Mazhari, S.A., Bea, F., Amini, S., Ghalamghash, J., Molina, J.F., Montero, P., Scarrow, J.H. & Williams, I.S., 2009. The Eocene bimodal Piranshahr massif of the Sanandaj–Sirjan Zone, NW Iran: a marker of the end of the collision in the Zagros Orogen. *Journal of the Geological Society* 166, 53–69.

McCulloch, M.T. & Chappell, B.W., 1982. Nd isotopic characteristics of S- and I-type granites. *Earth and Planetary Science Letters* 58, 51–64.

Mehdipour Ghazi, J. & Moazzen, M., 2015. Geodynamic evolution of the Sanandaj-Sirjan Zone, Zagros Orogen, Iran. *Turkish Journal of Earth Sciences* 24, 513–528.

Middlemost, E.A.K., 1994. Naming materials in the magma/igneous rock system. *Earth-Science Reviews* 37, 215–224.

Moghadam, H.S., Li, X.H., Ling, X.X., Stern, R.J., Santos, J.F., Meinhold, G., Ghorbani, G. & Shahabi, S., 2015. Petrogenesis and tectonic implications of Late Carboniferous A-type granites and gabbronorites in NW Iran: Geochronological and geochemical constraints. *Lithos* 212–215, 266–279.

Mohajjel, M. & Fergusson, C.L., 2014. Jurassic to Cenozoic tectonics of the Zagros Orogen in northwestern Iran. *International Geology Review* 56, 263–87.

Mohajjel, M., Fergusson, C.L. & Sahandi, M.R., 2003. Cretaceous – Tertiary convergence and continental collision, Sanandaj–Sirjan Zone, western Iran. *Journal of Asian Earth Sciences* 21, 397–412.

Monfaredi, B., Hauzenberger, C., Neubauer, F., Schulz, B., Genser, J., Shakerardakani, F. & Halama, R., 2020. Deciphering the Jurassic–Cretaceous evolution of the Hamadan metamorphic complex during Neotethys subduction, western Iran. *International Journal of Earth Sciences* 109, 2135–2168.

Moradi Noghondar, M., Karimpour, M., Farmer, G. & Stern, C., 2011. Sr-Nd isotopic characteristic, U-Pb zircon geochronology, and petrogenesis of Najmabad Granodiorite batholith, Eastern Iran. *Journal of Economic Geology* 3, 27–145.

Mortimer, N., Hoernle, K., Hauff, F., Palin, J.M., Dunlap, W.J., Werner, R. & Faure, K., 2006. New constraints on the age and evolution of the Wishbone Ridge, southwest Pacific Cretaceous microplates, and Zealandia–West Antarctica breakup. *Geology* 34, 185–188.

Pearce, J., 1983. Role of the Sub-Continental Lithosphere in Magma Genesis at Active Continental Margins [In:] C.J. Hawkesworth, & M.J. Norry (Eds): *Continental Basalts and Mantle Xenoliths*. Shiva, Nantwich, 230–249.

Pearce, J.A., Harris, N.B.W. & Tindle, A.G., 1984, Trace element discrimination diagrams for the tectonic interpretation of granitic rocks. *Journal of Petrology* 25, 956–983.

Peccerillo, A. & Taylor, S.R., 1976. Geochemistry of Eocene calc-alkaline volcanic rocks from the Kastamonu area, Northern Turkey. *Contributions to Mineralogy and Petrology* 58, 63–81.

Raeisi, D., Mirnejad, H. & Sheibi, M., 2019. Emplacement mechanism of the Tafresh granitoids, central part of the Urumieh–Dokhtar Magmatic Arc, Iran: evidence from magnetic fabrics. *Geological Magazine* 156, 1510–1526.

Ricou, L.E., 1994. Tethys reconstructed: plates continental fragments and their boundaries since 260 Ma from Central America to South-eastern Asia. *Geodinamica Acta* 7, 169–218.

Safarzadeh, E., Masoudi, F., Hassanzadeh, J. & Pourmoafi, S.M., 2016. The presence of Precambrian basement in Gole Gohar of Sirjan (south of Iran). *Iranian Journal of Petrology* 7, 153–170.

Sepahi, A.A., Shahbazi, H., Siebel, W. & Ranin, A., 2014. Geochronology of plutonic rocks from the Sanandaj-Sirjan zone , Iran and new zircon and titanite U-Th-Pb ages for granitoids from the Marivan pluton. *Geochronometria* 41, 207–215. doi:10.2478/s13386-013-0156-z.

Sepahi, A.A., Salami, S., Lentz, D., McFarlane, C. & Maanijou, M., 2018. Petrography, geochemistry, and U–Pb geochronology of pegmatites and aplites associated with the Alvand intrusive complex in the Hamedan region, Sanandaj–Sirjan zone, Zagros orogen (Iran). *International Journal of Earth Sciences* 107, 1059–1096.

Shabanian, N., Reza, A., Dong, Y. & Liu, X., 2018. U-Pb zircon dating, geochemistry and Sr-Nd-Pb isotopic ratios from Azna-Dorud Cadomian metagranites,

Sanandaj-Sirjan Zone of western Iran. *Precambrian Research* 306, 41–60.

Shahbazi, H., Siebel, W., Pourmoafee, M., Ghorbani, M., Sepahi, A.A., Shang, C.K. & Abedini, M.V., 2010. Geochemistry and U – Pb zircon geochronology of the Alvand plutonic complex in Sanandaj – Sirjan Zone (Iran): New evidence for Jurassic magmatism. *Journal of Asian Earth Sciences* 39, 668–683.

Shakerardakani, F., Neubauer, F., Genser, J., Masoudi, F. & Mehrabi, B., 2015. Tectonic history of the central Sanandaj-Sirjan zone, Iran: Potentially Permian to Mesozoic polymetamorphism and implications for tectonics of the Sanandaj-Sirjan zone. *EGU General Assembly* 17.

Sheikholeslami, M.R., 2015. Deformations of Palaeozoic and Mesozoic rocks in southern Sirjan, Sanandaj–Sirjan Zone, Iran. *Journal of Asian Earth Sciences* 106, 130–149.

Soesoo, A., 2000. Fractional crystallization of mantle□derived melts as a mechanism for some I□type granite petrogenesis: an example from Lachlan Fold Belt, Australia. *Journal of the Geological Society* 157, 135 LP – 149.

Stampfli, G.M. & Borel, G.D.. 2002, A plate tectonic model for the Paleozoic and Mesozoic constrained by dynamic plate boundaries and restored synthetic oceanic isochrons. *Earth and Planetary Science Letters* 196, 17–33.

Tahmasbi, Z., Castro, A., Khalili, M. & Khalaji, A.A., De, J., 2010. Petrologic and geochemical constraints on the origin of Astaneh pluton, Zagros. *Journal of Asian Earth Sciences* 39, 81–96.

Takahashi, M., Aramaki, S. & Ishihara, S., 1980. Magnetite-series/ilmenite series vs. I-type/S-type granitoids, granitic magmatism and related mineralization. *Mining Geology* 8, 13–28.

Tarkian, M., Lotfi, M. & Baumann, A., 1983. *Tectonic, magmatism and the formation of mineral deposits in the central Lut, east Iran*. Ministry of Mines and Metals, GSI, geodynamic project (Geotraverse) in Iran, No. 51.

Tavakoli, N., Davoudian, A.R., Shabanian, N., Azizi, H., Neubauer, F., Asahara, Y. & Bernroider, M., 2020. Zircon U-Pb dating, mineralogy and geochemical characteristics of the gabbro and gabbro-diorite bodies, Boein–Miandasht, western Iran. *International Geology Review* 62, 1658–1676.

Teknik, V. & Ghods, A., 2017. Depth of magnetic basement in Iran based on fractal spectral analysis of aeromagnetic data. *Geophysical Journal International* 209, 1878–1891.

Whalen, J.B., Currie, K.L. & Chappell, B.W., 1987. A-type granites: geochemical characteristics, discrimination and petrogenesis. *Contributions to Mineralogy and Petrology* 95, 407–419.

Wu, F., Sun, D., Li, H., Jahn, B. & Wilde, S., 2002. A-type granites in northeastern China: age and geochemical constraints on their petrogenesis. *Chemical Geology* 187, 143–173.

Yajam, S., Montero, P., Scarrow, J., Ghalamghash, J., Razavi, S. & Bea, F., 2015. The spatial and compositional evolution of the Late Jurassic Ghorveh-Dehgolan plutons of the Zagros Orogen, Iran: SHRIMP zircon U-Pb and Sr and Nd isotope evidence. *Geologica Acta* 13, 25–43.

Yang, T.N., Chen, J.L., Liang, M.J., Xin, D., Aghazadeh, M., Hou, Z.Q. & Zhang, H.R., 2018. Two plutonic complexes of the Sanandaj-Sirjan magmatic-metamorphic belt record Jurassic to Early Cretaceous subduction of an old Neotethys beneath the Iran microplate. *Gondwana Research* 62, 246–268.

Zhang, H., Chen, J., Yang, T., Hou Z. & Aghazadeh, M., 2018a. Jurassic granitoids in the northwestern Sanandaj – Sirjan Zone : Evolving magmatism in response to the development of a Neo-Tethyan slab window. *Gondwana Research* 62, 269–286.

Zhang, Z., Xiao, W., Ji, W., Majidifard, M.R., Rezaeian, M., Talebian, M., Xiang, D., Chen, L., Wan, B., Ao, S. & Esmaeili, R., 2018b. Geochemistry, zircon U-Pb and Hf isotope for granitoids, NW Sanandaj- Sirjan zone, Iran: Implications for Mesozoic-Cenozoic episodic magmatism during Neo-Tethyan lithospheric subduction. *Gondwana Research* 62, 227–245.

Zhao, X.-F., Zhou, M.-F., Li, J.W. & Wu, F.Y., 2008. Association of Neoproterozoic A- and I-type granites in South China: Implications for generation of A-type granites in a subduction-related environment. *Chemical Geology* 257, 1–15.

Manuscript submitted: 16 August 2021
Revision accepted: 25 February 2022